COO-3077-146
MF-90

Courant Institute of
Mathematical Sciences

Magneto-Fluid Dynamics Division

MHD Stability for a Class of Tokamak Equilibria with Fixed Boundary

W. Kerner

U.S. Energy Research and Development Report

Plasma Physics
August 1977

New York University

UNCLASSIFIED

New York University

Courant Institute of Mathematical Sciences

Magneto-Fluid Dynamics Division

MF-90 COO-3077-146

MHD STABILITY FOR A CLASS OF TOKAMAK EQUILIBRIA WITH FIXED BOUNDARY

W. Kerner

August 1977

U.S. Energy Research and Development Administration

Contract No. EY-76-C-02-3077*000

UNCLASSIFIED

Abstract

The stability behavior with respect to internal modes is discussed for a class of tokamak equilibria with non-circular cross-sections and essentially flat current profiles. The stability analysis is performed numerically with the help of a normal mode code, which extremizes the Lagrangian of the system. It is found that the Mercier criterion is both necessary and sufficient for stability. Strong numerical evidence for this result is given. MHD-stable high-beta equilibria exist in this model.

Introduction

The ideal magnetohydrodynamic (MHD) approximation for describing a plasma is very useful for understanding present tokamak experiments and for designing new devices. In this paper we present results obtained from a computer code which solves for the complete spectrum of normal modes. The method consists in extremizing the Lagrangian of the system connected with linearized perturbations around an equilibrium configuration using a Galerkin procedure [1].

The class of equilibria is characterized by a pressure profile, $p = p_o - p'\psi$, and a poloidal current profile, $T \equiv XB_\phi = R \left[B_o^2 + 2 \psi \delta p'/(1 + a^2) \right]^{1/2}$, with p_o, p', B_o, δ, α as constants. The flux function ψ is given by

$$(1) \qquad \psi = p' \left[Z^2 (X^2 - R^2\delta) + \alpha^2 (X^2 - R^2)^2/4 \right]/2(1 + \alpha^2).$$

Here R is the radius of the magnetic axis and X,ϕ,Z denote the usual cylindrical coordinate system. The stability analysis is performed in a non-orthogonal flux coordinate system ψ,ϕ,Θ. For details, we refer to [1 - 4]. The toroidal current density is

$$(2) \quad j_\phi = p'(X - R^2\delta'/X (1 + \alpha^2))$$

and the (contravariant) poloidal current density j^Θ is

$$(3) \quad j^\Theta = \tilde{X} \alpha \delta R^2 (p')^2/T (1 + \alpha^2)^2,$$

with

$$(4) \quad X = (R^2 + 2 \psi \cos \Theta)^{1/2} , \quad \tilde{X} = (X^2 - R^2\delta)^{1/2}$$

Near the magnetic axis, $\psi = 0$, the flux surfaces are ellipses with a half-axis ratio

(5) $e = \alpha / (1 - \delta)^{1/2}$

and become Dee-shaped further outward.
The condition that the flux surfaces are all closed within the plasma region imposes the following restrictions

(6) $\psi_b/R^2 < 1/2$ and $\psi_b/R^2(1 - \delta) < 1/2$,

where ψ_b denotes the value at the plasma boundary. The inverse aspect ratio ε is approximately given by

(7) $$\varepsilon = \psi_b/R^2$$

The method and the first application of the code are published in [1]. The main results can be summarized as follows: Toroidal effects are destabilizing for free surface modes, i.e. the conducting wall is far away from the plasma. The stability of internal modes, however, is improved by the toroidicity. Another application of our code has been to provide an independent check of the general Princeton equilibrium and stability code [5] and of the Lausanne Code [6]. A careful comparison of the results has given confidence in all three approaches and will be reported elsewhere.

In previous publications concerning our equilibrium model, [1,6,7], only a few configurations, viz. $\delta = 0$ and $\alpha = 1,2$, or 4, are treated. In this paper we discuss the stability behavior of the full class of equilibria for modes which leave the plasma boundary unperturbed. We consider only non-axisymmetric perturbations, i.e. $n \neq 0$ in eq. (8). In particular the connection of gross modes with

the stability limit of a necessary (Mercier) criterion [8, 9] is discussed. In addition, it is examined whether MHD-stable high-beta equilibria exist.

Discussion

The normal mode approach has the property that the lowest eigenvalue is always approximated from above as the number of expansion functions is increased. No instability is then found for a stable system. It is our experience that with the set of global Fourier-Bessel expansion functions,

$$(8)\quad \underset{\sim}{\xi}\,(\underset{\sim}{r},t) = e^{-i\omega t}\, e^{in\phi}\, X^2 \tilde{X} \sum_{l,\nu} C_{l,\nu}\, \underset{\sim}{\xi}_{l,\nu}(\psi)\, e^{il\theta} \quad ,$$

sufficient accuracy is obtained with 9 to 11 Fourier components and 5 or 6 radial expansion functions; see [1]. An extrapolation to infinitely many expansion functions only changes the eigenvalues by 1 - 5 % in most cases. For L Fourier components and M radial functions the numerical results indicate that the eigenvalue ω^2 converges as

$$\omega_o^2 - C_L \exp(-\alpha_L L),$$

with $\alpha_L \sim 1$ for fixed M,

and as $\omega_o^2 - C_M \exp(-\alpha_M M)$ for fixed L, with α_L, α_M, C_L and C_M constants. Up to 15 Fourier components and 6 global functions have been used. This leads to 270 x 270 matrices in the eigenvalue problem. Such a case needs about 3 minutes CPU time on the NYU CDC 6600 computer.

In order to discuss the connection with localized modes, we note that the strongest restriction on the safety factor from Mercier's criterion [8, 9] is given in the neighborhood of the magnetic axis, see [2]. Therefore, we do not evaluate Mercier's criterion numerically, but use an approximation given by Lortz and Nührenberg [10] which is valid for small values of the inverse aspect ratio ε. The value of the safety factor at the axis, $q(o)$, necessary for stability is then given by

$$(9)\quad 1/q^2(o) < 6/1+e^2 - 4/e(e+1) + Q\,[\,4/e(e+1) - 2\,],$$

where $Q = -\delta/(1+\alpha^2 - \delta)$.

An approximation for the plasma beta, valid for small ε, has the form

$$(10)\quad \beta_T = \frac{1+\alpha^2}{2}\ \frac{\varepsilon^2}{q^2(o)\ (1-\delta)}$$

and

$$(11)\quad \beta_p = \frac{1+\alpha^2}{1+\alpha^2-\delta}\ .$$

From the localized criterion of eq. (9) we get a restriction on the possible beta values:

$$(12)\quad \beta_T \leq \frac{1+e^2(1-\delta)}{2}\ \frac{\varepsilon^2}{1-\delta}\left\{\frac{6}{1+e^2} - \frac{4}{e(e+1)} - \frac{\delta}{(1-\delta)\ (1+e^2)}\,[\,4/e(e+1) - 2\,]\right\}.$$

Equation (12) shows that an optimization with respect to beta can be obtained by choosing configurations with noncircular cross-sections ($e \geq 1$) and diamagnetic current distributions ($\delta > o$).

The value for the plasma beta is especially high if the parameter δ is chosen close to unity but compatible with eq. (6), i.e. $1-\delta > 2\varepsilon$. We then obtain for the toroidal and poloidal plasma beta

$$(10b)\quad \beta_T = \frac{1+e^2\cdot 2\varepsilon}{4}\qquad \varepsilon/q^2(o)$$

and

$$(11b)\quad \beta_p = \frac{1+e^2\cdot 2\varepsilon}{2(1+e^2)}\qquad \varepsilon^{-1}$$

We emphasize that all configurations have nonvanishing magnetic shear. The magnitude of this shear is given by the inverse aspect ratio and the poloidal current, i.e. by the parameters ε and δ. Only the cylindrical limit is shearless. In Table I we give the ratio of q on surface to q on axis for different values of ε and δ. A typical q profile is plotted in Fig. 1. In the following discussion we present results for configurations with large aspect ratios, $\varepsilon^{-1} = 10$, and small aspect ratios, $\varepsilon^{-1} = 4$ and 3. Here, n and l denote the toroidal and poloidal wave numbers in eq. (8). We sometimes denote as l_o the dominant Fourier component in the poloidal direction Θ. The eigenvalues are normalized to the poloidal Alfvèn speed

$$\Omega^2 = \omega^2\, \rho_o\, \psi_b{}^2\, (1+\alpha^2)/2\, R^2\, p_o(1-\delta),$$

with a constant plasma density ρ_o.
A strong MHD instability with $\Omega^2 \approx -1$ corresponds to a timescale of the order of microseconds, a weak instability with $\Omega^2 \approx -10^{-6}$ to milliseconds.

Large Aspect Ratio, $\varepsilon^{-1} = 10$

For a quantitative comparison between the stability limit of localized and gross modes the critical q(o) from eq. (9) is plotted in Fig. 2 as a function of the elongation e for different values of δ.

A system with $q(o)$ greater than $q(o)_{cr}$ is stable with respect to localized perturbations.

The first interesting result is that for an almost circular cross-section, $e = 1$, no unstable $n = 1$ mode exists. This holds for all values of α and δ with $e \equiv \alpha/(1-\delta)^{1/2} = 1$. This result is in agreement with [6,7]. The critical safety factor from the necessary criterion has the value $q(o)_{cr} = 1$. This stability limit is approached by modes with a toroidal wave number $n \to \infty$ and a dominant Fourier component $l_o = n - 1$. Then instabilities exist for $q(o) \simeq l_o/n = (n-1)/n$. We are able to find such unstable modes for $2 \leq n \leq 14$, as shown in Fig. 3.

The ϕ and θ integrations for evaluating the matrix elements in δL are done very accurately by means of an extensive algebraic calculation [1, 18]. No difficulty is then caused by the fact that for a case with $n = 14$ and 15 Fourier components centered around $l_o = 14$ the poloidal wave number l varies between 7 and 21. A different method with a numerical θ integration, however, requires a special procedure for such high l numbers . The eigenvalues for $2 \leq n \leq 8$ are quite accurate, at least up to 5 %. The range of instability $\Omega^2 = \Omega^2(q)$ in Fig. 3 does not change significantly when more functions are included. For higher n values, $n \geq 10$, more exspanion functions are necessary for convergence. It is very likely that a mode with $n = 20$, $l_o = 19$ will require 20 Fourier components or more for a correct representation. But in no case does an instability disappear with an increasing number of expansion functions.

Instead of determining the stability boundary in terms of q for a given elongation, we now determine the critical elongation when q(o) and n are kept fixed. We begin with the fundamental mode n = 1. The safety factor is chosen as q(o) = 1. The results for the corresponding cylindrical equilibria, [11, 12, 13], indicate that the interesting mode should basically be a n = 1 and l_o = 1 mode. The growth rates computed as a function of e for values of δ=-2, -1, 0, 0.5, 0.75 are shown in Fig. 4a. In Table II the computed critical elongations for marginal stability are listed. The two marginal points e_{cr} define an interval in e with stability with respect to the n = 1 mode. These values agree well with the localized criterion, eq. (9) and Fig. 2. The critical safety factor from the necessary criterion is evaluated for the computed e_{cr} and also listed in Table II. The agreement with the chosen value q(o) = 1 is again very good.

Next we examine the growth rates for values of e close to e_{cr}. It is seen from Fig. 4 that the eigenvalues of the unstable modes drop one or two orders of magnitude before the marginal point is reached. The slope of the function $\Omega^2 = \Omega^2(e)$ is almost zero for $e = e_{cr}$ and the eigenvalues in the stable region are very close to zero. Since the continuous part of the spectrum extends for n = 1, l_o = 1 and q(o) = 1 up to the origin with eigenvalues Ω^2 proportional to $(n\, q(\psi_s) - 1)^2$, this behavior is indeed correct.

At this point we want to discuss the numerical accuracy again. The results stated are obtained with 11to15 Fourier components and 6 radial expansion functions. Increasing the number of expansion functions further would

shift the marginal points only a little to even better agreement with the necessary criterion. Especially, the inclusion of more radial functions will produce stable modes with growth rates closer to zero.

In order to discuss further details, it is instructive to look at the corresponding eigenfunctions. The eigenfunctions of the dominant Fourier component $1_o = 1$ for $n = 1$, and $1_o = 2$ for $n = 2$, are plotted in Figs. 5 and 6 for a case with $\delta=-1$. Here $\xi^1(\psi) = R\,\xi^\psi$ and $\xi^3(\psi) = \psi\,\xi^\Theta/R$ denote contravariant components. The ξ^ϕ component is too small to be shown. The contribution of the other Fourier components is at least one order of magnitude smaller, with the exception of the $1_o \pm 1$ components. Here only the toroidal component ξ^ϕ is present. This coupling is due to toroidal effects and can be explained by studying the spectrum at the origin, [14]. Assuming $|\xi^\psi| << \partial/\partial_\psi |\xi^\psi|$, the marginal points of the potential energy are defined by the following equations (see also [4]):

(13) $n\,q - 1_o = 0,$

(14) $\nabla \cdot \underline{\xi} = 0,$

(15) $\nabla \cdot \underset{\sim}{\xi}_\perp / X^2 = 0.$

Here $\underset{\sim}{\xi}_\perp$ denotes the part of the displacement vector perpendicular to the magnetic field.

Combining eqs. (14) and (15) and using eq. (4) leads to

$$\frac{\partial}{\partial\psi} X^2 = 2\cos\Theta\,, \qquad \frac{\partial}{\partial\Theta} X^2 = -2\psi\sin\Theta.$$

The marginal point for the perturbed toroidal field, Q_ϕ, then yields the condition

$$(15)\quad \sum_e e^{il\Theta} \left[(n\,q - 1)\,\xi_l^\phi + F_{l+1}^- + F_{l-1}^+\right] = 0,$$

with $F_e^\pm = \xi_l^\psi \pm \psi\ \xi_l^\Theta$.

Evaluating eq. (15) shows that $\xi^\phi_{l_o \pm 1}$ is of the order of $\xi^\psi_{l_o}$ and $(\psi\xi^\Theta_{l_o})$, and that $\xi^\psi_{l_o \pm 1}$ and $(\psi\xi^\Theta_{l_o \pm 1})$ are small and hence $\xi^\phi_{l_o}$ is as well.

It is seen from Fig. 5, 6 that the eigenfunctions are gross modes similar to the straight system eigenfunctions, but vanish in the outer part of the plasma, where the shear is strongest. If q(o) is chosen smaller than 1.0 the eigenfunctions now extend in the radial direction up to the plasma boundary, as can be seen from Figs. 5 and 6. More then one instability, corresponding to eigenfunctions with several radial modes, exist. The shape of the eigenfunctions does not depend much on whether e is close to e_{cr} or not. Generally, instabilities exist for a mode with wave numbers n and l_o if n q(o) has values between $l_o - \eta_1$ and $l_o + \eta_2$ with constants η_1, η_2 ($\eta_1 \neq \eta_2$). But, if for an unstable mode the elongation e approaches the value e_{cr}, the interval in q(o) for which instabilities occur shrinks to one point $q(o) = n/l_o$. For $n = 1$ and $l_o = 1$ this point is q(o) = 1. This is shown in Fig. 7. According to Mercier [15] such a configuration with e = 1 is marginally stable for q(o) = 1. The numerical evaluation of the Mercier criterion for finite ε even indicates stability for q(o) = 1. Hence, the considered $n = 1$, $n_o = 1$ mode, would be unstable in a Mercier stable region. The conclusion based on the numerical evidence is that the Mercier criterion is also sufficient for stability. This result is confirmed by many runs of the code with

different values of n and q(o) where the parameters α and δ are varied. The results from a similar analysis for n = 1 and q(o) = 2.0 are shown in Fig. 4b and Table II. Note that for elliptical cross-sections more Fourier terms are necessary for convergence.

Pao [16] has shown that an n = 1 and 1_o = 1 instability of a circular cylinder should also occur in the corresponding toroidal configurations. Because of the weak shear near the axis in our equilibrium model the singular region, which is assumed to be small in [16], is here of considerable radial extent and so this analysis cannot be applied here.

The region of stability with respect to the n = 1 mode can be enlarged by a suitable choice of the poloidal current. For a paramagnetic current distribution, $\delta < o$, the stable region occurs for $e < 1$, i.e. lying ellipses, and for diamagnetic ones, $\delta > o$, for standing ellipses. This stabilizing effect may be important for Belt Pinch devices with a possible increase in the plasma beta by factor of 5 to 10 compared with the circular cross-section (eqs. (10) - (12)).

Finally, all the information about stability can easily be obtained from eq. (9) and Fig. 2. For a chosen value of $q(o) = \hat{q}(o)$ the stable region for every value of α and δ can be seen. Furthermore, we know that the relevant modes have wave numbers n and 1_o with $n\,\hat{q}(o) - 1_o \simeq 0$. In the unstable region instabilities occur also for values of q(o) close to $\hat{q}(o)$, and more than one instability corresponding to eigenfunctions with several modes in the radial direction are found. This statement has also been checked and confirmed in detail for $\hat{q}(o) = 1.5$ and for an n = 2, 1_o = 3 mode.

Small Aspect Ratio $\varepsilon^{-1} = 4$ or 3

It is an important question whether additional instabilities occur if the aspect ratio is decreased. It turns out that toroidicity improves the stability behavior.

We again examine the n = 1 mode. For an almost circular cross-section, e = 1, this mode remains stable for small aspect ratio. For q(o) = 0.99 the critical elongation for marginal stability is listed in Table III. These values are very similar to the large aspect ratio cases with increased regions of stability.

We discuss in detail the stability of a JET-like configuration, e = 2, with two different values of β_p. The aspect ratio chosen is $\varepsilon^{-1} = 4$. For smaller values of ε^{-1} the parameter δ, restricted by $\delta < 1 - 2\varepsilon$, is essentially zero and hence $\beta_p = 1$.

The two cases differ in the stability boundary of the necessary criterion, $q_{cr} = 1.37$ for $\delta = o$ and $q_{cr} = 1.18$ for $\delta = 0.4$. The q profiles are plotted in Fig. 1. The growth rates of the unstable modes with n = 1,2,3, and 4 are plotted in Fig. 8. For configurations with e = 2 and q(o) = 1.0 the Mercier criterion is violated. Therefore, the n = 1 and $l_o = 1$ mode is unstable for both cases. For a toroidal wave number n = 2 the $l_o \geq 3$ modes with $q(o) \simeq l_o/n \geq 1.5$ are Mercier stable and, hence, these modes are found to be stable by the code. But the $l_o = 1$ and 2 modes are unstable and strongly coupled. Owing to the larger shear the $l_o = 1$ mode is shifted to smaller values of q(o) for $\delta = 0.4$ in comparison with $\delta = o$.

For n = 3 and $l_o = 4$ the safety factor $q(o) \simeq 4/3 = 1.33$ violates the necessary criterion for $\delta = o$ but satifies it for $\delta = 0.4$. Hence

the $l_o = 4$ mode is unstable in the case with $\delta = o$, but stable when $\delta = 0.4$. The $l_o = 3,2$ and 1 modes are unstable in both cases. For modes with $n = 4$ the results are similar. These results are reproduced for a smaller aspect ratio $\varepsilon^{-1} = 3$.

Note that the stabilizing influence of a diamagnetic current profile is now smaller, viz. $\delta < 1/3$. High-beta equilibria, which are MHD stable with respect to internal modes then exist according to eqs. (10) to(12).

Finally, it is interesting to note that for large elongations the sufficient criterion of [10] coincides with the necessary criterion. Configurations with lying ellipses, $e < 1$, as cross-sections are found to be highly unstable in our calculations in agreement with the Mercier criterion. Therefore, diamagnetic configurations with $\beta_p > 1$, which are unstable even if the Mercier criterion is satisfied, only seem likely for elongations with $1 < e < 3$. According to eq. (11b) the poloidal plasma beta is considerably smaller than ε^{-1}. This may be the reason why we do not see any ballooning-type modes ([17]).

Summary

The MHD stability is discussed for a class of analytic tokamak equilibria with essentially flat volume current profiles but with elliptical or Dee-shaped cross-sections. The normal modes of the system are computed using a Ritz-Galerkin procedure in the Langrangian formalism. The equilibria of this model are highly unstable with respect to external kink perturbations. But these instabilities can be

stabilized by a perfectly conducting wall placed on the plasma surface.

The basic result is that the Mercier criterion is necessary and sufficient for stability of fixed boundary modes for this entire class of tokamaks. By studying many different configurations strong numerical evidence, which leads to this result, is given. Since increasing the inverse aspect ratio always has a stabilizing effect, the stability limit is obtained from the necessary criterion evaluated near the magnetic axis.

The corresponding shearless, straight system equilibria are always unstable with respect to internal modes. The toroiodal configurations have small shear near the magnetic axis which rapidly increases only in the vicinity of the boundary. This feature implies that no cylinder-like region around the axis with instabilities in the Mercier stable domain of parameter space exists. The fact that the poloidal plasma beta cannot be increased arbitrarily but is considerably smaller than ε^{-1} may explain the absence of ballooning-type modes. Therefore, MHD-stable high-beta equilibria exist.

The study of other equilibria with peaked current profiles is planned for the future. We expect that a stabilizing effect on the external kink instabilities is connected with more internal instabilities. An interesting question then is whether the flattening of the current profile in some areas, e.g. around $q = 2$ and $q = 3$ surfaces, again has a beneficial effect on the internal modes.

References

[1] Kerner, W.; Nucl. Fus. 16 (1976), 643

[2] Küppers, G.; Pfirsch, D.; Tasso, H. in Plasma Physics and Controlled Nuclear Fusion Research (Proc. 4th Int. Conf. Madison, 1971) 2, IAEA, Vienna (1971) 529

[3] Kerner, W.; Tasso, H. in Plasma Physics and Controlled Nuclear Fusion Research (Proc. 5th Int. Conf. Tokyo, 1974) 1, IAEA, Vienna (1975) 475

[4] Kerner W, ; IPP 6/134, Garching, March (1975)

[5] R.C. Grimm,; J.M. Greene,; and J.L. Johnson in "Methods in Computational Physics", Vol 16, Academic Press, New York, 1976, 253

[6] D. Berger, L.C. Bernard, R. Gruber and F. Troyon in Plasma Physics and Controlled Nuclear Fusion 1976, IAEA, Vienna (1977) Paper CN-35/B11-4 (1976)

[7] Sykes, A.; Wesson, J.A. in Plasma Physics and Controlled Nuclear Fusion Research (Proc. 5th Int.Conf. Tokyo, 1974) 1, Vienna (1975) 449

[8] Mercier, C.; Nucl. Fusion 1 (1960) 47

[9] Greene, J.M.; Johnson, J.L; Phys. Fluids 5 (1962), 510

[10] Lortz, D.; Nührenberg, J.; Nucl. Fusion 13 (1973), 821

[11] Taylor, R.J.; Proc. Phys. Soc. London B70 (1957) 1043

[12] Chance, M.S.; Greene, J.M.; Grimm, R.C.; Johnson, J.L.; Nucl. Fusion 17 (1976), 53

[13] Berger, D.; Gruber, R.; Troyon, F.; Comp. Phys. Communications 11 (1976), 313

[14] Gruber, R.; private communication

[15] Mercier, C.; Nucl. Fusion 4 (1964), 213

[16] Pao, Y.P.; Phys. Fluids, 19, (1976), 1796

[17] Todd, A.M.; Chance, M.S., Greene, J.M.; Grimm, R.C., Johson, J.L.; Manickam, J.; Phys. Rev. Letters 38 (1977), 826

[18] Kerner, W.; Steuerwald, J. Comput. Phys. Comm. 9 (1975), 337

Table I

Ratio q_b/q_o (q on surface to q on axis)

δ	$\varepsilon^{-1} = 10$	δ	$\varepsilon^{-1} = 4$	δ	$\varepsilon^{-1} = 3$
-2	1.021	-2	1.16	-2	1.36
-1	1.025	1	1.19	-1	1.49
0	1.039	0	1.31	0	1.74
0.5	1.082	0.25	1.44	0.25	2.10
0.75	1.31	0.40	1.70	0.30	2.81

Table II

Numerical evidence of the sufficiency of the Mercier criterion

$\varepsilon^{-1} = 10$; $n = 1$

	$q(0) = 1.0$		$q(0) = 2.0$	
δ	$e_{cr.}$ (CODE)	$q_{cr.}$ (MERCIER)	$e_{cr.}$ (CODE)	$q_{cr.}$ (MERCIER)
-2	0.40	1.02	0.29	2.05
	1.015	1.008	2.42	2.02
-1	0.56	1.017	0.40	2.02
	1.013	1.003	2.60	2.013
0	0.93	1.005	0.60	2.02
	1.10	1.008	3.15	2.02
1/2	0.987	1.005	0.78	2.02
	1.66	1.003	4.16	2.03
3/4	0.985	1.02	0.86	2.10
	2.60	1.02	5.92	2.10

Table III

Numerical evidence of the sufficiency of the Mercier criterion

$n = 1, \quad q(0) = 0.99$

ε^{-1}	δ	e_{cr}(CODE)		q_{cr}(MERCIER)
4	0	0.91	1.09	1.01
	0.4	0.97	1.15	1.01
3	0	0.90	1.11	1.01
	0.25	0.94	1.30	1.02

Figure Captions

Fig. 1 q profiles for $\varepsilon^{-1} = 4$

Fig. 2 Mercier criterion near axis

Fig. 3 Growth rates of unstable internal modes for $\varepsilon^{-1} = 10$, $\alpha = 1$, $\delta = 0$

Fig. 4 Eigenvalues versus ellipticity

a) $\varepsilon^{-1} = 10$, n = 1, q(0) = 1.0

b) $\varepsilon^{-1} = 10$, n = 1, q(0) = 2.0

Fig. 5 Eigenfunctions for n = 1, $l_o = 1$ modes

$\xi^1 \equiv R\xi^{\psi}$, $\xi^3 = \psi\, \xi^{\Theta} / R$

$\varepsilon^{-1} = 10$, $\delta = -1$, e = 0.53

a) q(0) = 1.0, $\Omega^2 = -0.18 \times 10^{-5}$

b) q(0) = 0.997, $\Omega^2 = -0.22 \times 10^{-5}$

c) q(0) = 0.994, $\Omega^2 = -0.9 \times 10^{-6}$

Fig. 6 Eigenfunctions for n = 1, $l_o = 2$ modes

$\xi^1 \equiv R\xi^{\psi}$, $\xi^3 = \psi\, \xi^{\Theta} / R$

$\varepsilon^{-1} = 10$, $\delta = -1$, e = 0.53

a) q(0) = 1.0, $\Omega^2 = -0.5 \times 10^{-5}$

b) q(0) = 0.997, $\Omega^2 = -0.8 \times 10^{-5}$

c) q(0) = 0.994, $\Omega^2 = -0.4 \times 10^{-5}$

Fig. 7 Eigenvalues versus safety factor

$\varepsilon^{-1} = 10$

a) n = 1, $\delta = -1$

b) n = 2, $\delta = -1$

c) n = 1, $\delta = 0.75$

Fig. 8 Growth rates versus safety factor

$\varepsilon^{-1} = 4$, e = 2

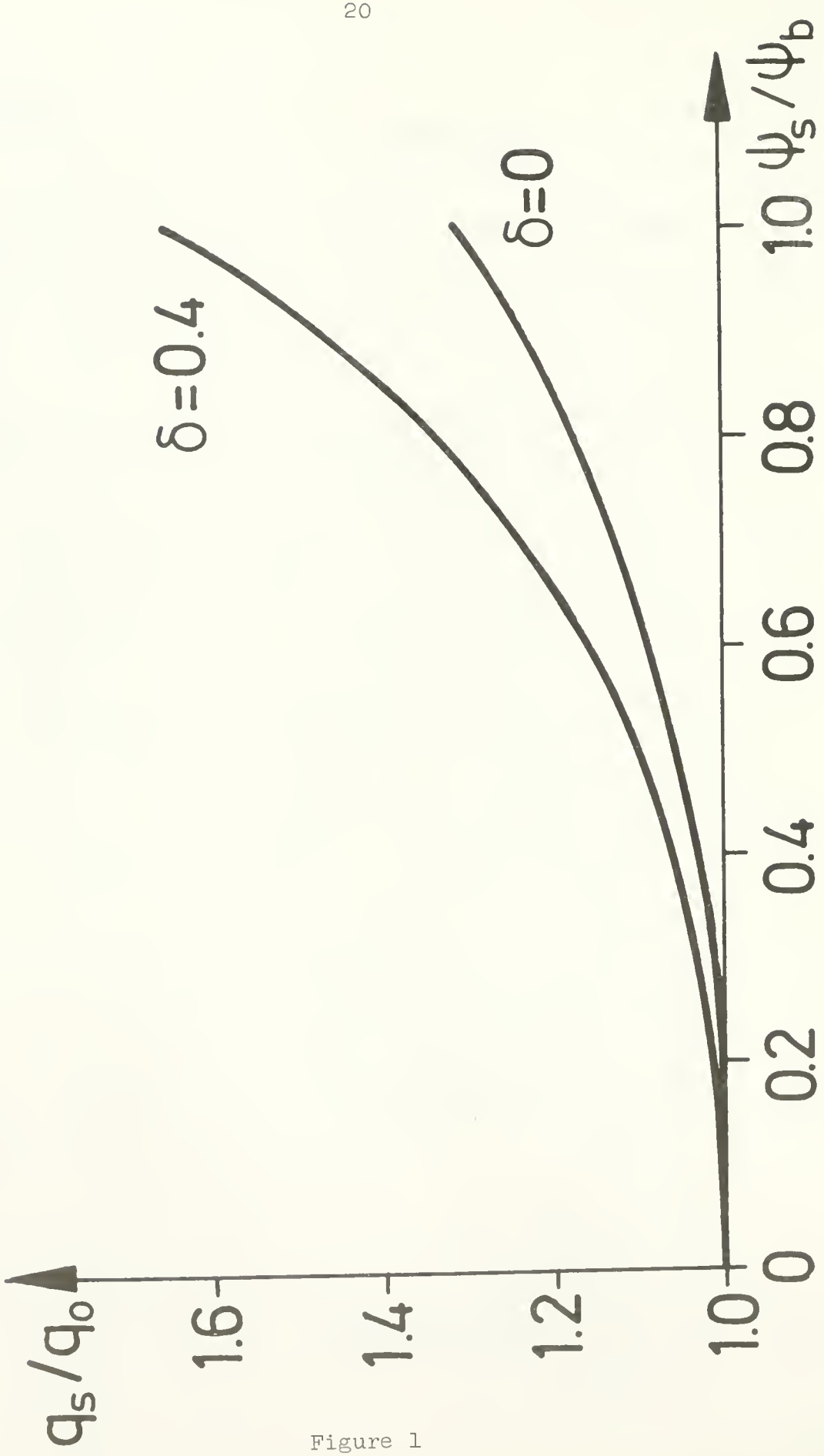

Figure 1

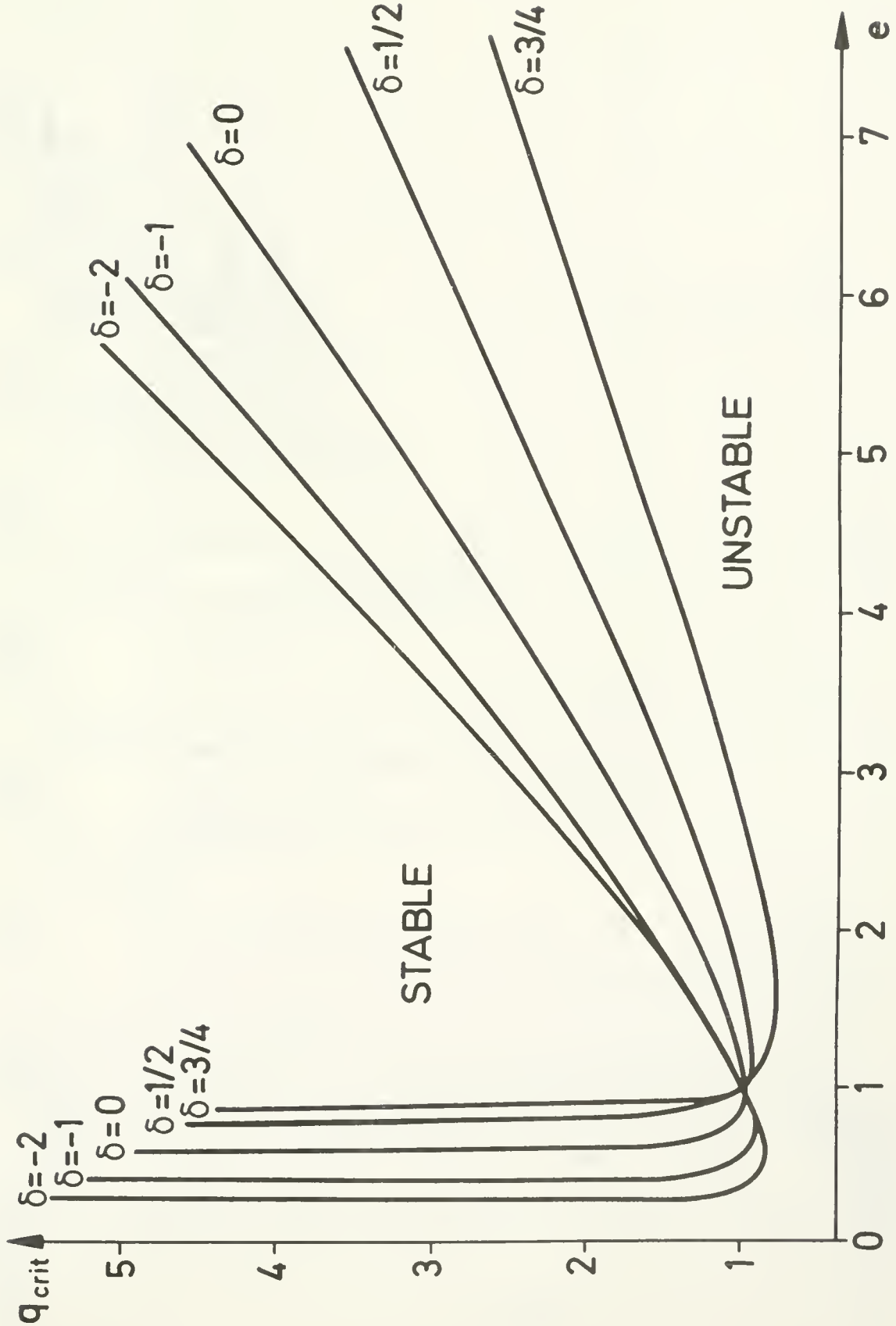

Figure 2

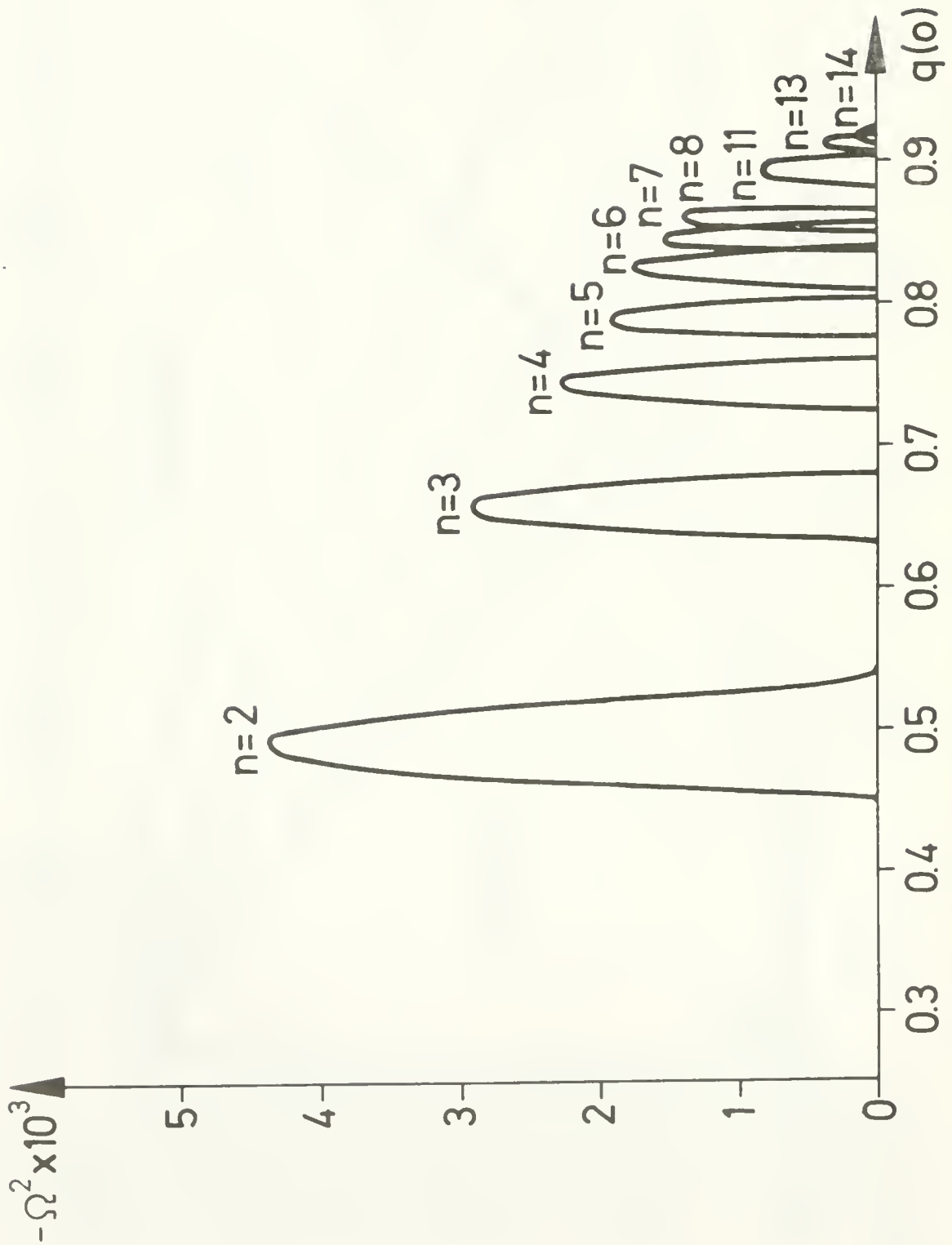
$-\Omega^2 \times 10^3$
5
4
3
2
1
0
0.3
0.4
0.5
0.6
0.7
0.8
0.9
q(o)
n=2
n=3
n=4
n=5
n=6
n=7
n=8
n=11
n=13
n=14

Figure 3

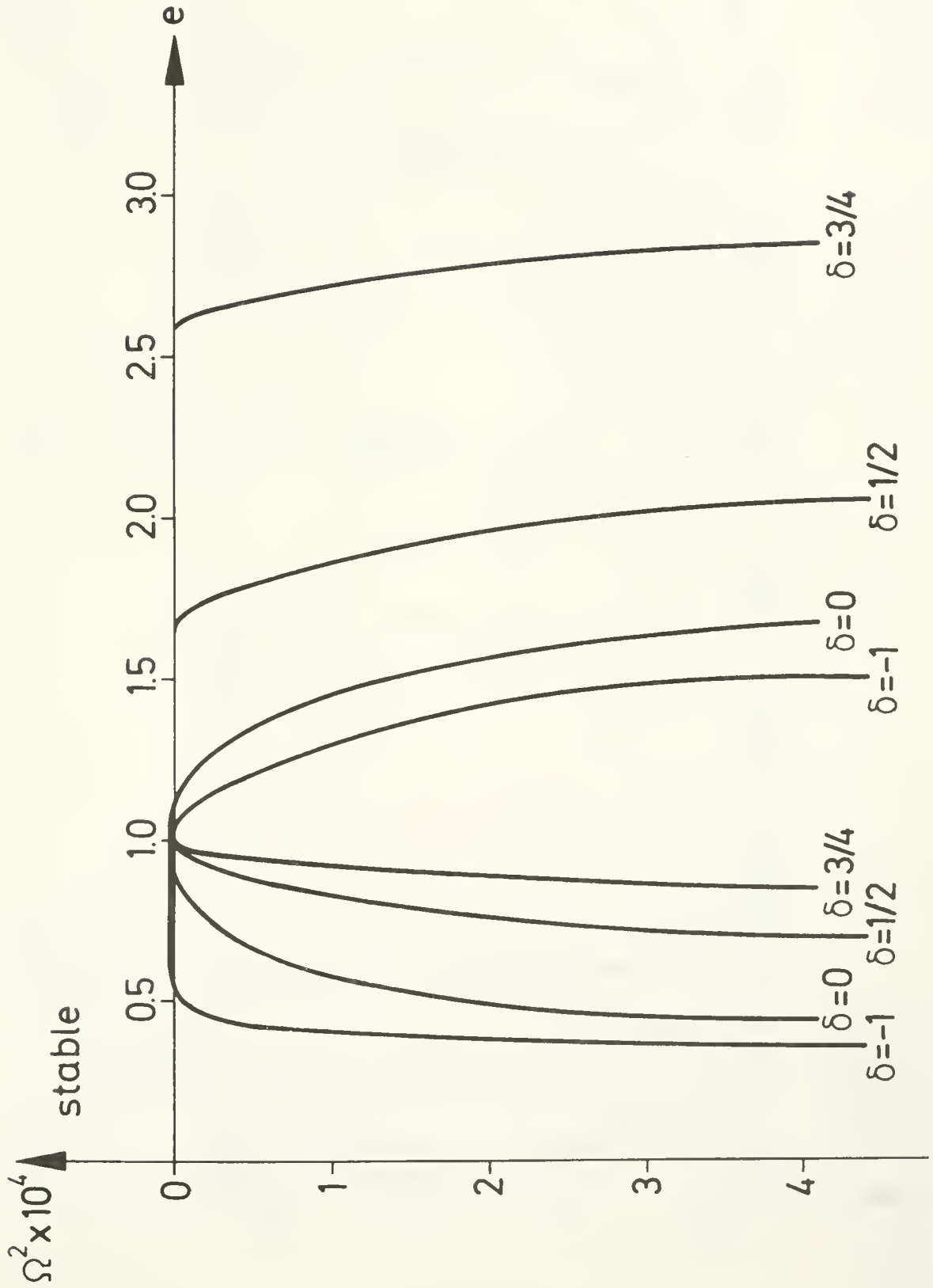
e
3.0
2.5
2.0
1.5
1.0
0.5
stable
$\Omega^2 \times 10^4$
0
1
2
3
4
δ=3/4
δ=1/2
δ=0
δ=-1
δ=3/4
δ=1/2
δ=0
δ=-1

Figure 4a

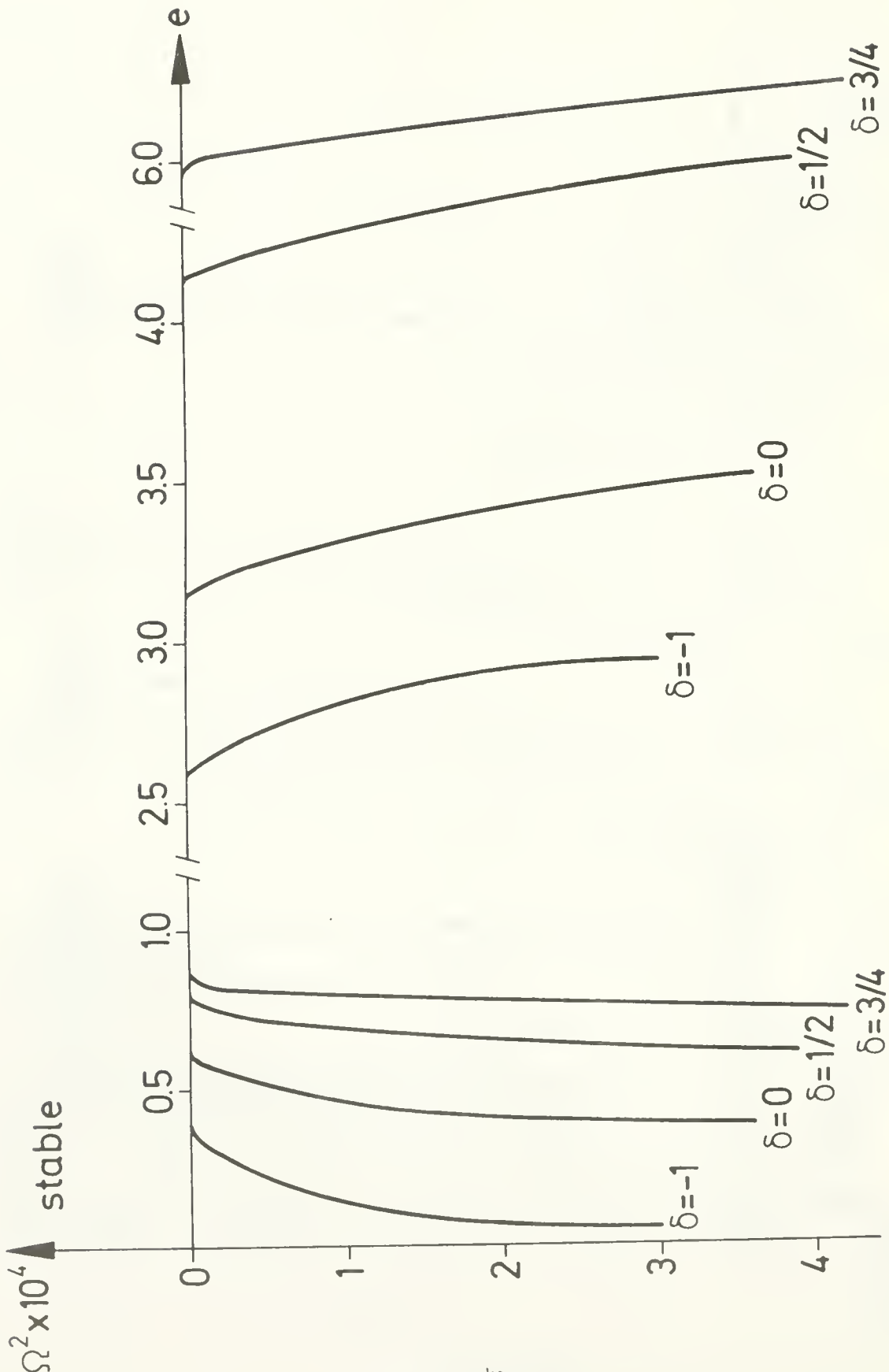
e
6.0
4.0
3.5
3.0
2.5
1.0
0.5
stable
$\Omega^2 \times 10^4$
0
1
2
3
4
δ=3/4
δ=1/2
δ=0
δ=-1
δ=3/4
δ=1/2
δ=0
δ=-1

Figure 4b

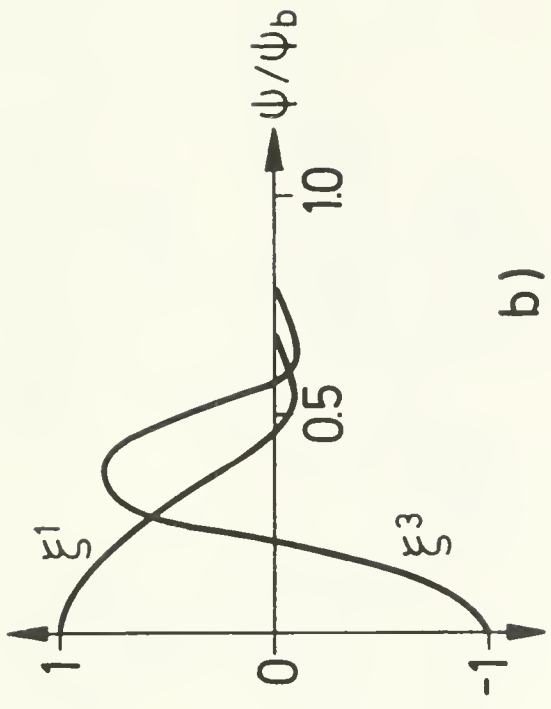

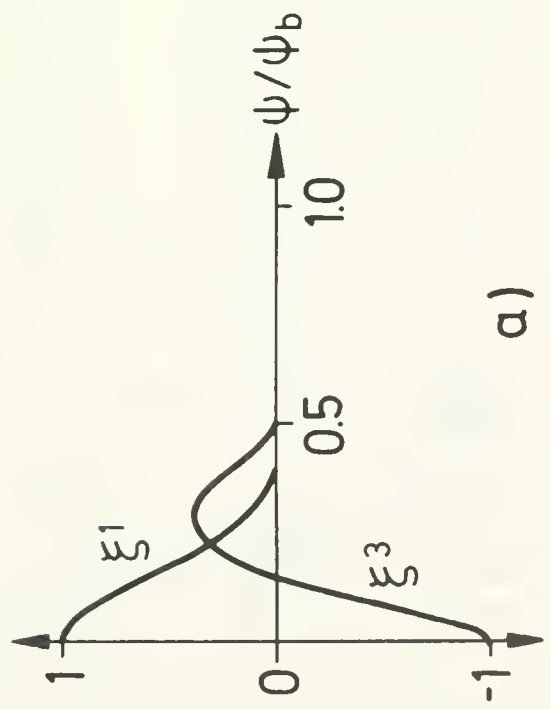

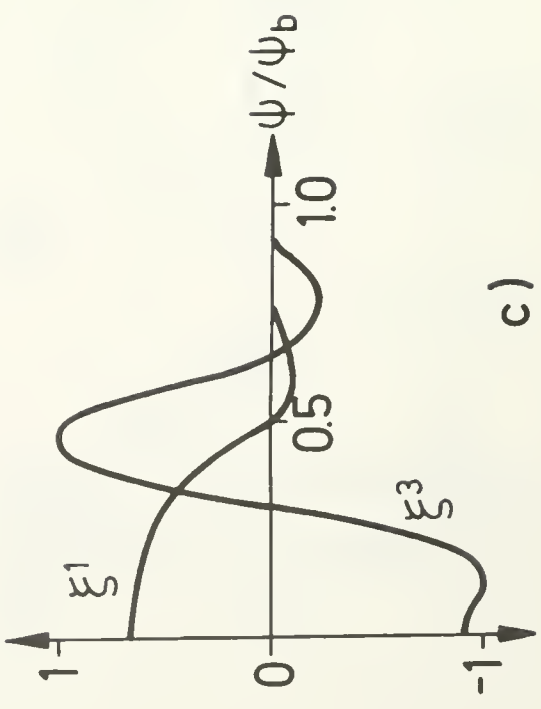

Figure 5

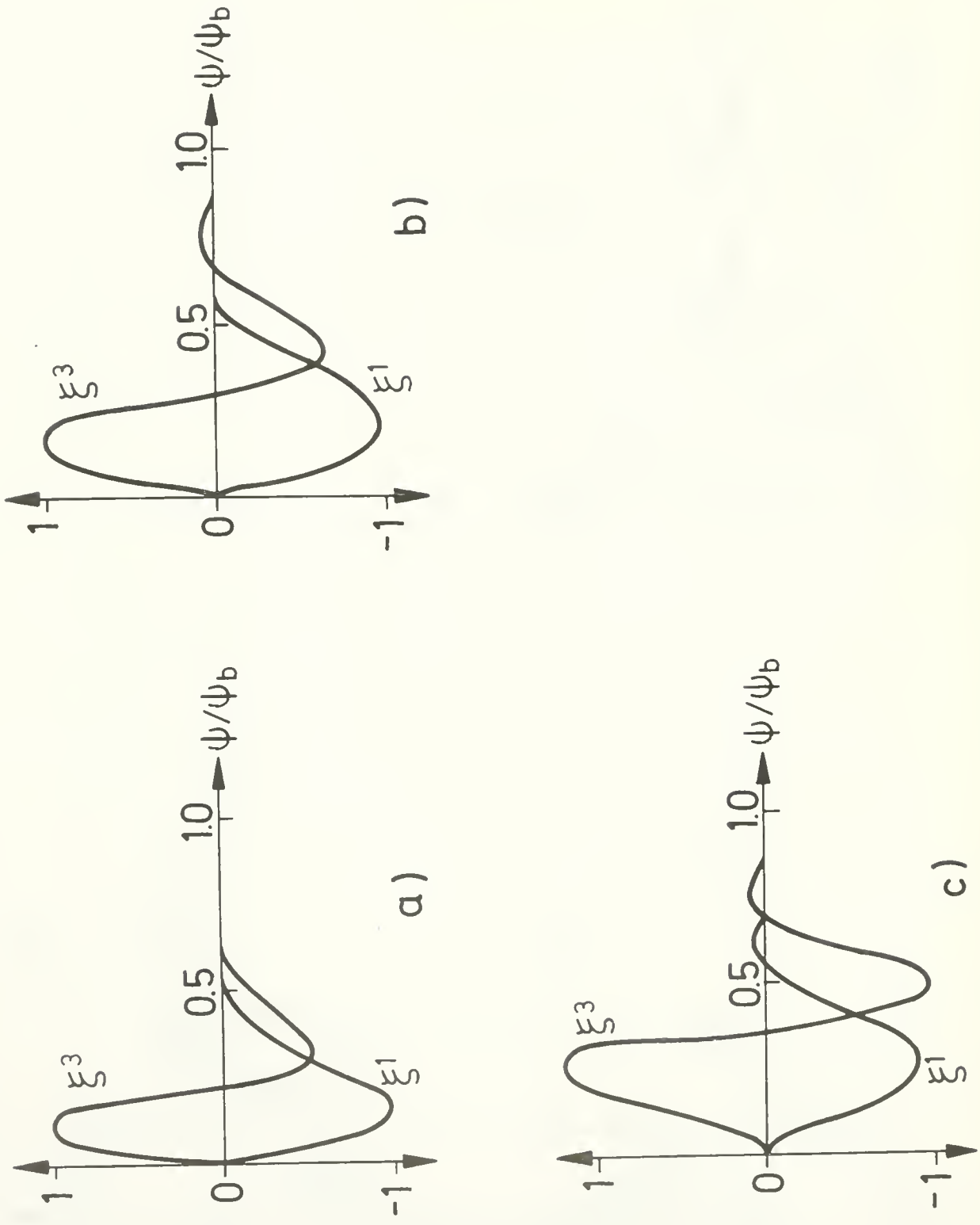

Figure 6

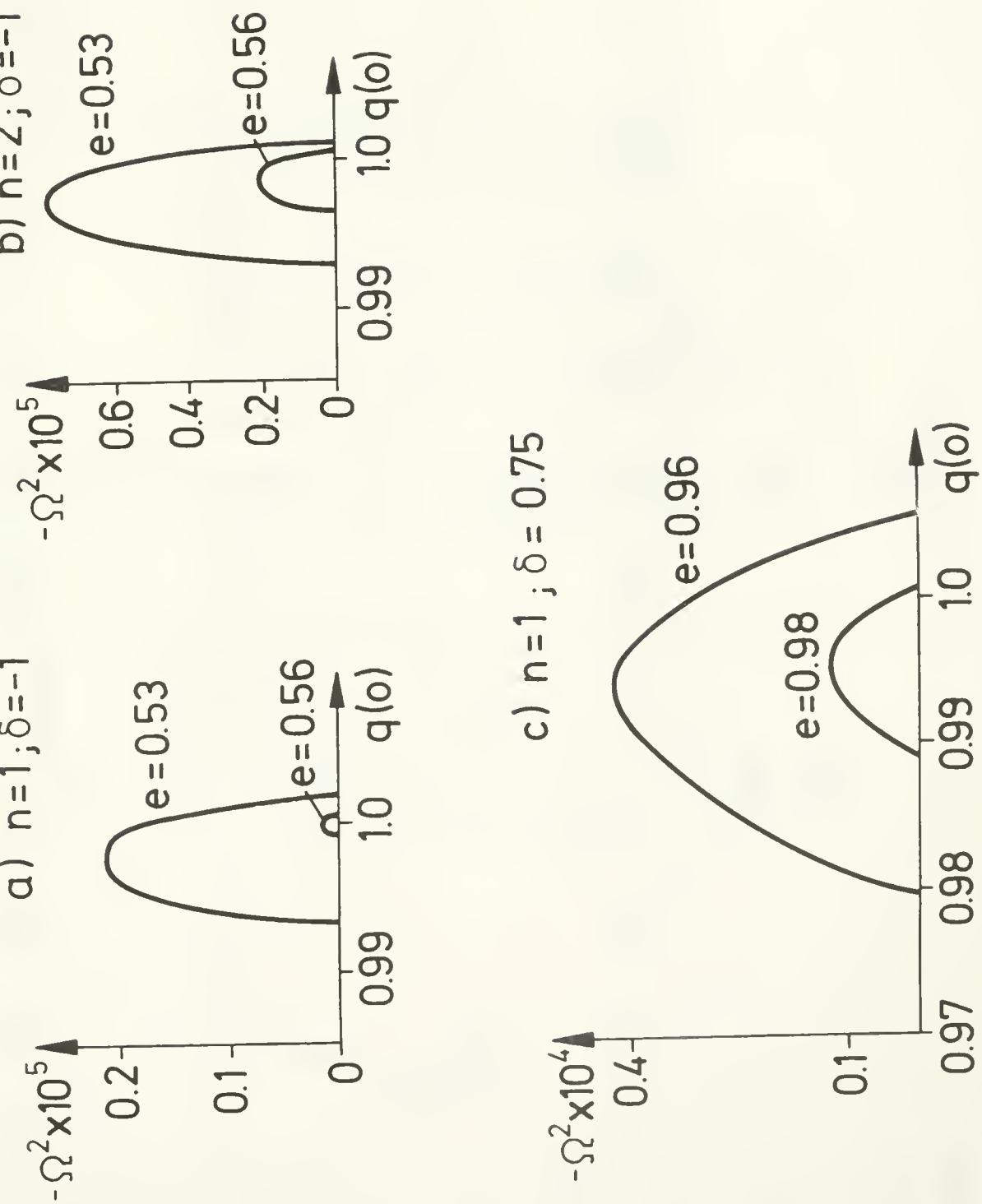
a) n=1; δ=-1
b) n=2; δ=-1
c) n=1 ; δ= 0.75
e=0.53
e=0.56
e=0.96
e=0.98
$-\Omega^2 x10^5$
$-\Omega^2 x10^4$
0.2
0.1
0
0.6
0.4
0.99
1.0
q(o)
0.97
0.98

Figure 7

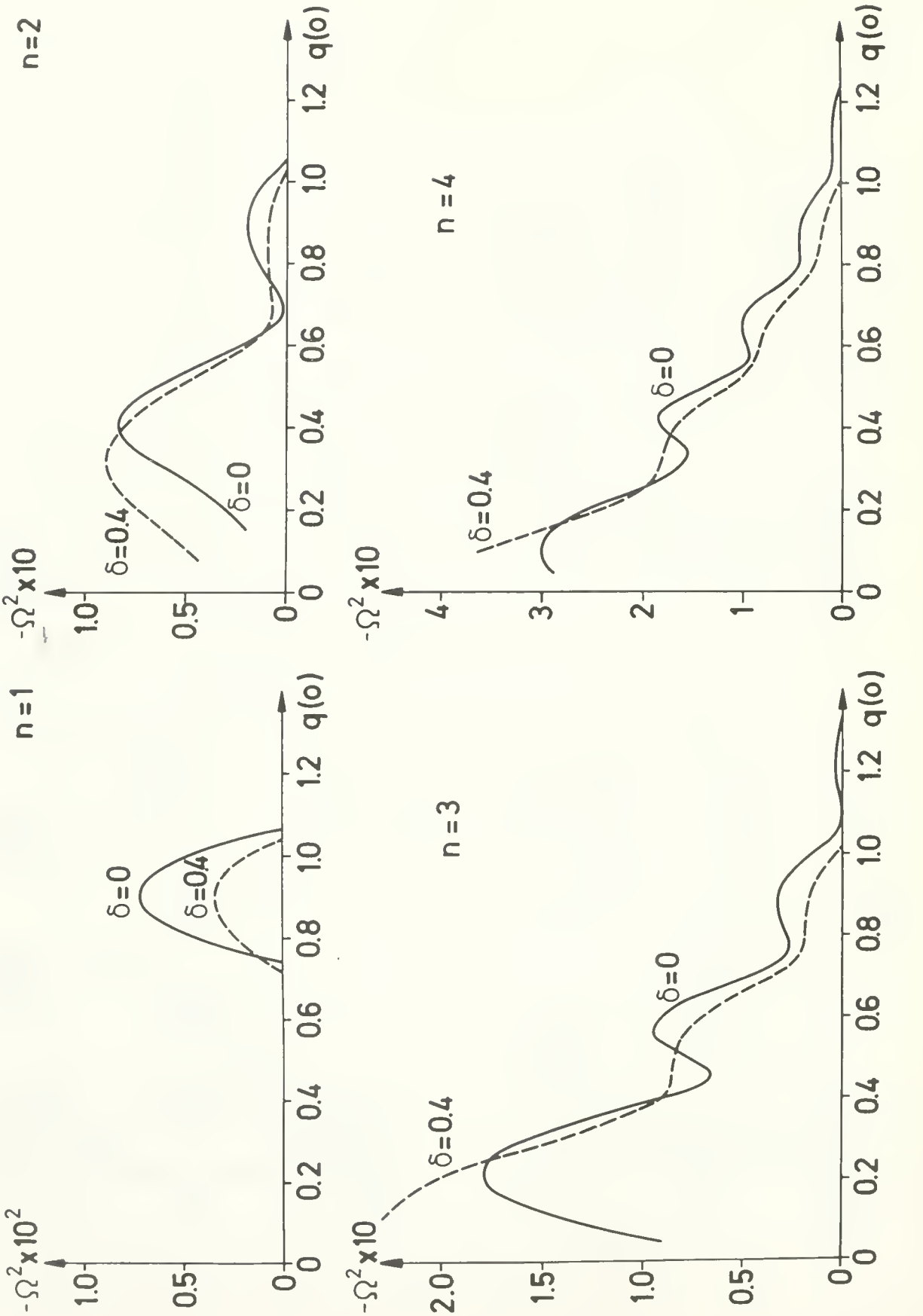
n=1
n=2
n=3
n=4
δ=0
δ=0.4
$-\Omega^2 x10^2$
$-\Omega^2 x10$
q(o)
0
0.2
0.4
0.6
0.8
1.0
1.2
0.5
1.5
2.0
1
2
3
4

Figure 8

This report was prepared as an account of Government sponsored work. Neither the United States, nor the Administration, nor any person acting on behalf of the Administration:

A. Makes any warranty or representation, express or implied, with respect to the accuracy, completeness, or usefulness of the information contained in this report, or that the use of any information, apparatus, method, or process disclosed in this report may not infringe privately owned rights; or

B. Assumes any liabilities with respect to the use of, or for damages resulting from the use of any information, apparatus, method, or process disclosed in this report.

As used in the above, "person acting on behalf of the Administration" includes any employee or contractor of the Administration, or employee of such contractor, to the extent that such employee or contractor of the Administration, or employee of such contractor prepares, disseminates, or provides access to, any information pursuant to his employment or contract with the Administration, or his employment with such contractor.